Nonlinear dynamics of lava dome extrusion

O. Melnik*† & R. S. J. Sparks*

** Centre for Environmental and Geophysical Flows, Department of Earth Sciences, University of Bristol, Bristol BS8 1RJ, UK*
† Institute of Mechanics, Moscow State University, 1 Mitchurinski prosp, 117192, Moscow, Russia

During the eruption of the Soufrière Hills volcano, Montserrat (1995–99), and several other dome eruptions, shallow seismicity, short-lived explosive eruptions and ground deformation patterns indicating large overpressures (of several megapascals) in the uppermost few hundred metres of the volcanic conduit have been observed. These phenomena can be explained by the nonlinear effects of crystallization and gas loss by permeable flow, which are here incorporated into a numerical model of conduit flow and lava dome extrusion. Crystallization can introduce strong feedback mechanisms which greatly amplify the effect on extrusion rates of small changes of chamber pressure, conduit dimensions or magma viscosity. When timescales for magma ascent are comparable to timescales for crystallization, there can be multiple steady solutions for fixed conditions. Such nonlinear dynamics can cause large changes in dome extrusion rate and pulsatory patterns of dome growth.

Lava dome eruptions involve the ascent of gas-rich magmas, which lose gas during ascent[1]. Degassing results in rheological stiffening[2,3] due to gas exsolution and microlite crystallization from undercooled melt. Viscosity can increase by several orders of magnitude when silicic melts containing a few per cent dissolved water decompress and degas[4]. Microlite crystallization from undercooled melt accentuates the viscosity increase[5], and can lead to the magma changing isentropically into a hot crystalline solid with mechanical strength. Crystallization of microlites and gas loss by permeable flow are time-dependent processes that introduce strong nonlinearities into the dynamics of conduit flow and dome extrusion. Here we develop a model of conduit and lava extrusion which incorporates these processes. The nonlinear behaviour identified in our calculations provide explanations for some important features observed in the eruption of the andesite lava dome of the Soufrière Hills, Montserrat, including ground deformation patterns, shallow seismicity, occurrence of short-lived vulcanian explosions, and large fluctuations of magma discharge rate. The model is, however, generic and can also explain phenomena at other eruptions, such as Mount Unzen in Japan.

Model development

Models of lava extrusion[6] commonly involve application of the Poiseuille flow law. Here extrusion rate is inversely proportional to the viscosity, proportional to the conduit width raised to some power (4 for a cylinder), and proportional to the pressure gradient. But this model is too simple for the study of intermediate and silicic magmas, because of the rheological stiffening that accompanies degassing and the variable density of vesiculating magma. Many aspects of these complications have already been considered. Gas loss by permeable flow to the conduit walls can cause nonlinear variations in flow rate and transitions between explosive and extrusive activity[7,8]. These transitions are very sensitive to small changes in parameter values, and the system of equations that incorporates gas loss can produce multiple solutions. Large viscosity variations related to gas loss cause strongly nonlinear pressure gradients and overpressures (defined here as the difference between magma pressure and local lithostatic pressure) at high levels in the conduit[2]. Microlite crystallization can also potentially cause large overpressures to develop in the uppermost several hundred metres of conduits[2,9].

The physical framework for our model is shown in Fig. 1. Magma is stored in a chamber at depth L with a chamber overpressure, P_c, defined as chamber pressure minus lithostatic pressure, initial magma viscosity μ_0 and mass concentration of water dissolved in the melt phase of c_0. The magma ascends along a cylindrical conduit of diameter D and exits at the vent with pressure P_e. Flow in the dome is represented by a continuation of the conduit, with the same diameter for the active zone of flow within the dome and extrusion of new lava at the summit, consistent with observations at the Soufrière Hills volcano[10]. This simplification does not alter the underlying principles that emerge from our calculations. During ascent of the magma up the conduit and through the dome, gas is exsolved and is lost by vertical permeable flow through the magma column. In contrast to previous models[7,8], we consider only vertical gas flux. Although some gas loss to the conduit walls is inevitable, the observations of a strong gas plume emerging from the summit area of the Soufrière Hills dome[11] suggest that vertical flux is dominant. Sealing of the conduit walls also can prevent lateral gas loss[12,13].

We model the system shown in Fig. 1 by the following system of equations:

$$(1-\alpha)(\rho_m(1-\beta)(1-c)+\rho_c\beta)V = Q_m \quad (1)$$

$$\rho_m(1-\alpha)(1-\beta)cV + \rho_g\alpha V_g = Q_g \quad (2)$$

$$V\frac{d\beta}{dz} = \beta^{2/3}\frac{\chi}{\mu_m}\left(1-\frac{c}{c_0}\right); \quad \chi = 4\pi\left(\frac{3}{4\pi N}\right)^{2/3}\xi \quad (3)$$

$$\frac{dp}{dz} = -\rho g - \frac{32\mu V}{D^2} \quad (4)$$

$$V_g - V = -\frac{k(\alpha)}{\mu_g}\frac{dp}{dz} \quad (5)$$

$$\mu = \theta(\beta)\mu_m(c); \quad c = C_f\sqrt{p}; \quad p = \rho_g RT \quad (6)$$

$$\log[k(\alpha)/k_0] = -10.2(\alpha 10^2)^{1.4\times 10^{-2}\alpha^{-1}}; \quad \alpha > 0.03 \quad (7)$$

$$\log[\theta(\beta)/\theta_0] = \arctan[\omega(\beta-\beta_*)] + \pi/2 \quad (8)$$

where ρ_m, ρ_c and ρ_g are the densities of melt, crystals and gas, respectively, ρ is the density of mixture, α and β are volume concentrations of respectively bubbles and crystals (in the condensed phase), V and V_g are velocities of magma and gas, respectively, Q_m and Q_g are discharge rates of respectively magma and gas per unit area, p is pressure, c is the mass concentration of dissolved gas, μ, μ_m and μ_g are viscosities of magma, melt and gas, respectively, D is the conduit diameter, C_f is the solubility constant,

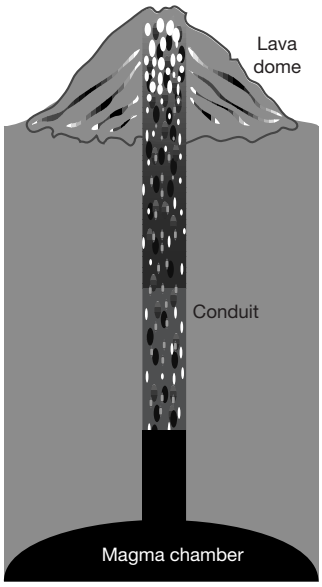

Figure 1 Schematic view of the volcanic system. Magma ascends from a chamber connected with the growing lava dome by a cylindrical conduit. Flow in the dome is represented by a continuation of the conduit, with extrusion of new lava at the summit of the dome. Gas is lost by permeable flow along the conduit near the surface.

Table 1 Parameters for the Sourfrière Hills andesite eruption used in modelling

Parameter	Symbol	Value range	Information sources
Magma chamber depth	L	5 km	Earthquakes[32] and phase equilibria[33]
Magma chamber pressure	P_c	0–20 MPa	Range of crustal strengths
Melt water content	c_0	5%	Ref. 33
Magma temperature	T	850 °C	Refs 25, 33
Magma crystal content	β_0	0.6	Ref. 25
Conduit diameter	D	30 m	Dimensions of spines and early crater; hornblende reaction rims[34]
Viscosity coefficient	θ_0	1.6	From calculations
Viscosity coefficient	β_*	0.62	From calculations
Viscosity coefficient	ω	20.6	From calculations
Crystal growth rate coefficient	χ	7×10^{-3} s^{-1}	From calculations
Permeability coeffcient	k_0	1	Regression through data
Density of melt	ρ_m	2,300 kg m^{-3}	
Density of crystals	ρ_c	2,700 kg m^{-3}	
Density of wallrock	ρ_r	2,600 kg m^{-3}	
Solubility coefficient	C_f	4.1×10^{-6} Pa$^{1/2}$	
Gas viscosity	μ_g	1.5×10^{-5} Pa s	

$k(\alpha)$ is the permeability, R is the gas constant, T is temperature, z is the vertical coordinate, g is the acceleration due to gravity, N is the number density of crystals per unit volume, ξ is a constant related to crystal growth kinetics, and k_0, ω, β_*, θ_0 are constants in permeability and viscosity laws as discussed below. Function $\theta(\beta)$ represents the influence of crystals on magma viscosity. Equations (1) and (2) represent conservation of mass for gas and condensed phase, and equation (3) describes crystal growth kinetics. Equation (4) states the conservation of momentum for the mixture in which the inertial term is negligibly small and conduit resistance is taken in Poiseuille form. Equation (5) is Darcy's law, and equations (6–8) summarize the physical properties of magma for isothermal flow conditions.

We recognize that this model is not a complete description, as there may still be important processes that have not been incorporated. The calculations, for example, assume that the ascent is sufficiently slow that the gas phase in the system is in equilibrium (that is, diffusion of gas into the bubbles is not rate-limiting). More elaborate models can be developed which incorporate disequilibrium in the gas phase, more realistic treatment of gas and magma movement in the dome and lateral pressure gradients in the conduit. To illustrate the principles of the model and to test the results on a well documented eruption, we have chosen parameters based on the Soufrière Hills andesite lava dome eruption (Table 1). We have also carried out sensitivity studies to establish how variations in important parameters listed in Table 1 affect the results.

We have made measurements of the matrix permeability and porosity of samples from the Soufrière Hills eruption with porosities in the range of 0 to 70%. These and other data[14] can be described by equation (7) with most data falling between curves for $k_0 = 1$ and $k_0 = 10$. Most of the porosity consists of interconnected vesicles in the residual glass phase, which is continuously distributed between crystalline phases. We consider, in agreement with the conclusions of Klug and Cashman[14], that there have been only minor changes in permeability due to cooling. As lava domes are highly fractured, the actual permeability in the upper parts of the conduit and dome may be even higher so we consider $k_0 = 100$ in addition to the impermeable end-member case ($k_0 = 0$). We will show *a posteriori* that the influence of permeable gas loss on extrusion rate is small for a wide range of k_0.

The influence of crystals on viscosity is given by equation (8), and an empirical formula which reproduces the expected shape of the relationship between crystal content and viscosity across the transition region where crystals become close-packed, as observed in experiments[5].

We have chosen a simple parameterization of crystal growth (equation (3)) based on theoretical and experimental studies[15,16] in which growth rate is proportional to undercooling and inversely proportional to melt viscosity. Both degree of undercooling and melt viscosity are dependent on dissolved gas content, and are thus strongly dependent on pressure. We assume for simplicity that there is a single crystal nucleation event, that is, N and χ are constants in equation (3). For magma viscosity we have taken the relevant magma parameters for the Soufrière Hills andesite (Table 1), and have applied experimentally based algorithms[4,5]. Very large changes in magma viscosity occur when the crystal content reaches a threshold value at the condition of close packing[5]. There are considerable uncertainties in assessing the appropriate threshold crystal content for natural magmas, as the melt fraction at the close-packed condition is dependent on both crystal shape[5] and grain size distribution[17].

There are two remaining problems in choosing parameters: that the crystal growth parameter, χ, and the viscosity coefficient $\theta(\beta)$, are not well constrained. Although there are some experimental data on crystal growth, none of the available data are sufficiently close to a natural system to provide a robust value of χ. The high crystal content of the Soufrière Hills magma in the chamber (estimated at 60–65%) means that the magma is close to conditions of close-packing. There are no experimental data that can help constrain this parameter accurately, yet the results of calculations are likely to be sensitive to the choice of $\theta(\beta)$ in equation (8). We therefore use observations of dome height, extrusion rate, and crystal content from the Soufrière Hills to calibrate values of χ and $\theta(\beta)$ to provide the basis for a more extensive investigation of the effects of the nonlinearities on flow. We note that the choice of rheological parameters are such that the viscosity of the Soufrière Hills andesite has a variation consistent with independent estimates made from petrological models[4] and observations of dome growth rates.

Feedback mechanisms are evident in the mathematical description. Lower magma permeability results in a decrease in the overall

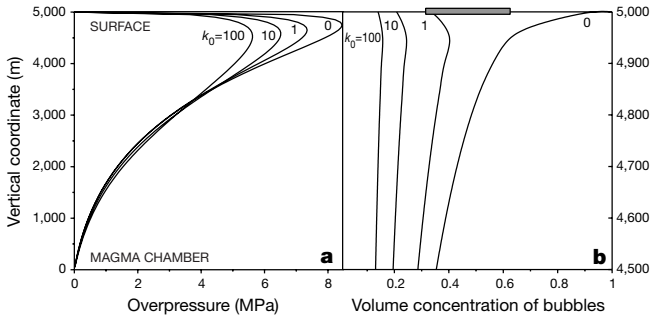

Figure 2 Calculated profiles of overpressure (**a**) and porosity (**b**) along a conduit. Conditions for calculations are described in the text. Overpressure (the difference between the magma pressure and lithostatic pressure) reaches a maximum in the uppermost few hundred metres of a volcanic conduit. Curves are shown for values of the permeability coefficient k_0 from values of 0 to 100. The range of observed porosities in pumice clasts from vulcanian eruptions of the Soufrière Hills is shown as a horizontal bar at the top of **b**. These data suggest that values of k_0 from 1 to 0.1 are typical. Low values of k_0 give unrealistically high porosities at the top of the conduit and explosive conditions are likely to develop in practice. Porosity profiles are shown for the upper 500 m of the conduit. The calculations here assume no crystallization in the conduit ($\chi = 0$).

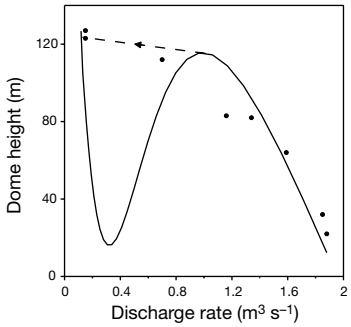

Figure 3 Calculated and observed magma discharge rate versus dome height. Shown are data for the October 1997 lava dome growth at Soufrière Hills volcano (filled circles), and the results of numerical calculations using equations (1)–(8). The dashed line shows the expected unsteady path for the system to change from one steady state to another with declining flow rate at approximately constant dome height: here the system cannot follow the steady path, because this would require a large decrease in dome height which is unphysical.

weight of the magma due to higher amounts of retained gas. The excess pressure driving magma from the chamber, defined as the difference between the chamber pressure and magma column weight, must consequently increase. As magma permeability increases, a larger proportion of the gas escapes, magma column weight increases, and the excess driving pressure decreases. Another example is the case when the timescale for magma extrusion is comparable to the timescale for microlite crystallization. If there is a slight change in some parameter that enhances flow rate (such as chamber pressure, conduit width or initial magma viscosity), then gas loss and crystallization will amplify the effect. An increase in flow rate will give less time for crystal growth, and so reduce overall viscosity. Also, an increase in flow rate gives less time for gas loss, therefore the magma column weight decreases. According to equation (4), the magma ascent velocity will consequently increase. We will show below that these feedback amplifications can be substantial.

Results of calculations and comparison with observations

We first demonstrate the influence of the permeability coefficient on eruption dynamics. Figure 2 illustrates the role of gas loss and permeability on flow dynamics, in terms of porosity and overpressure variations with depth. The calculations show a region of high porosity and high overpressure with a maximum in the uppermost parts of the conduit, at typical depths of a few hundred metres below the vent. The maximum overpressure depends on the permeability values, with a range of 4 to 8 MPa.

The model can explain, in the case of the Soufrière Hills, ground deformation patterns that indicate pressurization of the conduit rather than the deep magma chamber. Shepherd *et al.*[18] observed that deformation during 1996 could be described as a simple decrease in the velocity of ground movements radially away from the dome. They inferred a pressure source at 700 m depth with an estimated overpressure of 10 MPa. Voight *et al.*[3] estimated a pressure source at 400 m depth from cyclic patterns of ground inflation and deflation. Dome eruptions are characterized by shallow seismicity with long-period components[2,19,20], and by short-lived (a few tens of seconds) vulcanian explosions from shallow pressurized sources[3,9,20,21]. These phenomena can be explained by the predicted gas overpressures exceeding magma and conduit wallrock strength. Explosions occur when internal gas pressures exceed magma strength[22]. During the Soufrière Hill eruption, there were 85 vulcanian explosions in the August to October 1997 period[23]. Volume constraints indicate that these explosions originated from the uppermost few hundred metres of the conduit. Samples of the pumice had angular platy shapes indicative of brittle fragmentation and porosities of 30–60%, indicating a zone of high porosity and overpressures of a few megapascals, as predicted in the model. The calculated overpressures of several megapascals are comparable to the strength of the crystalline magma and wallrocks[22], so that the system is inherently unstable to perturbations such as unloading of the pressurized conduit by dome collapse. The cyclic patterns of seismicity, ground deformation, and eruptive activity documented by Voight *et al.*[3] can be seen as the consequence of pressurization repeatedly building up the system to failure conditions.

We now explore the effects of groundmass crystallization. Pumice and samples of the Soufrière Hills dome that were erupted during periods of high discharge[24] have high glass contents (25–35%) and few microlites[25], whereas samples derived from parts of the dome that were extruded more slowly (typically, days to weeks) have much lower glass contents (5–15%) and high contents of groundmass microlites. These, and other, observations[26–28] suggest that microlite crystallization can take place on similar timescales to the ascent time of the magma (see Table 1).

Figure 3 shows (as data points) the observed magma discharge rate versus dome height at the Soufrière Hills during October 1996. We first attempted to model the observations with flow models that did not include crystallization kinetics. Using data in Table 1 we were able to fit the initial discharge rate of 1.8 $m^3 s^{-1}$, but found that the ultimate height of the dome was much greater than observed (our best-fit value being about 600 m compared to 120 m). The height/discharge rate relationship could not be reconciled with the initial discharge rate at zero dome height: we therefore manipulated the controlling variables, and found values of χ and the constants in $\theta(\beta)$ that were consistent with the observations. The resulting calculated curve is shown in Fig. 3, and the parameter values are listed in Table 1. The model predicts strongly nonlinear behaviour when the height of the dome growth reaches about 120 m. At this point, dome growth cannot then follow the steady solution path as this requires a substantial decrease in height. Rather, we expect the dome to follow an unsteady path at approximately constant dome height until the curve for the steady solution is once more met at very low flow rate (Fig. 3). Large changes in extrusion rate have been observed with minor changes in dome height both at Soufrière Hills[24] and at Mount Unzen[20].

Figure 4 shows the relationship between extrusion rate and magma chamber overpressure, using values of χ and $\theta(\beta)$ determined from the dome growth in October 1997 (Fig. 3) and

contoured in terms of dome height from 0 to 300 m. The extrusion rate and heights cover the same range as observed at the Soufrière Hills eruption[24]. Figure 4b shows only the curves for 0 and 300 m dome height, and illustrates possible paths for eruption behaviour. Above a magma chamber pressure of 10 MPa the variations are monotonic, and the numerical results are close to the simple Poiseuille flow law. Extrusion rate decreases with dome height. In this region flow rates are too fast to allow significant crystallization. The slight departure from simple Poiseuille flow is due to the incorporation of gas loss by permeable flow.

For magma chamber overpressures below about 10 MPa the curves become more complex and sigmoidal in shape, indicating the possibility of multiple steady solutions for fixed eruption conditions. In this region, microlite crystallization occurs during ascent and introduces the strong feedback mechanisms described above. For low chamber overpressures (P_c) small changes in P_c can induce large changes in flow rate. We found similar strong sensitivity to small changes in conduit diameter or initial magma viscosity. For example, a change in viscosity or chamber pressure by a factor of two, or a 20% change of conduit width, can cause over an order of magnitude change in extrusion rate. The Poiseuille flow law would only result in a factor of 2 change.

The multiple steady solutions allow for complex pulsatory behaviour (Fig. 4b). A dome starting to grow at point A may reach 300 m height at point B. Beyond that height, the steady solution drops down to a much lower extrusion rate at point C. If the chamber pressure increases (for example due to magma replenishment[8]), then the path C, D, E can be followed and this might lead to periodic behaviour as the dome jumps between one steady state and another. A significant dome collapse event can decrease dome height suddenly, triggering greatly accelerated dome growth rates as shown in path E to F (Fig. 4).

Observations of dome growth at the Soufrière Hills[3,24] and Mount Unzen[20] showed pulsations on a wide range of timescales, from hours to months, with extrusion rates varying by a factor of more than 50. The composition of the magmas did not vary during the course of these eruptions, so variations in the initial magma crystal content and viscosity in the chamber are unlikely to have been a major cause of these pulsations and the large variations in extrusion rate. Relatively minor variations in the conduit dimensions and magma chamber pressure could have been amplified by the nonlinear effects to cause the wide range of extrusion rate and marked fluctuations.

The model we present here is limited by the need to calibrate it to a particular dome eruption; this is required to estimate poorly constrained parameters relating to the rheological properties of high-crystal-content magmas and crystallization kinetics. Although an independent estimate of the values of these parameters would be preferable, the choice of calibrated values allows us to learn about the general principles of nonlinear dynamics using values which are at least consistent with observations.

Implications for monitoring and forecasting

Our model of conduit flow and dome extrusion incorporates the nonlinear effects of degassing and crystallization. The calculations provide a mechanism for generating large overpressures at shallow levels in such eruptions. Evidence for overpressured conditions and pulsatory activity as characteristic of dome eruptions comes not only from the Soufrière Hills, but from elsewhere, such as Mount Unzen in Japan[20], Santiaguito in Guatemala[29], Lascar in Chile[21], Galeras in Columbia[9], and Mount St Helens in the USA[30]. The flow model introduces effects that help to explain ground deformation, shallow seismicity and short-lived vulcanian explosions. Cyclic patterns of behaviour, as at the Soufrière Hills[3], can be explained by build-up of overpressure in the upper parts of a conduit to critical threshold conditions for magma flow or explosive activity. Other mechanisms, such as stress weakening with stick–slip behaviour[31], may also play a role in short timescale cycles.

The model has important implications for the forecasting of volcanic eruptions. It suggests that many of the geophysical signals monitored in dome eruptions relate to pressurization in the upper parts of the conduit rather than the deep magma chamber. This link between flow models of degassing magma and monitoring data provides a new framework for interpretation of geophysical data.

Nonlinear dynamical effects allow multiple solutions to exist for fixed eruption parameters. Additionally, these eruptive systems can be extremely sensitive to minor changes in magma properties, magma chamber conditions and conduit dimensions. Unsteady transitions between stable states are themselves likely to prove of considerable interest. Nonlinear and unsteady behaviour makes possible transitions to chaotic behaviour as the system attempts to achieve equilibrium. Under some circumstances behaviour can become inherently unpredictable. Improved knowledge of crystal growth kinetics, gas exsolution kinetics (not incorporated here), permeability development in vesiculating magmas and rheological properties of crystal-rich magmas will help develop more complex and realistic models. However, nonlinearity will inevitably feature in future models, no matter how well constrained the eruption parameters and physical magma properties are. □

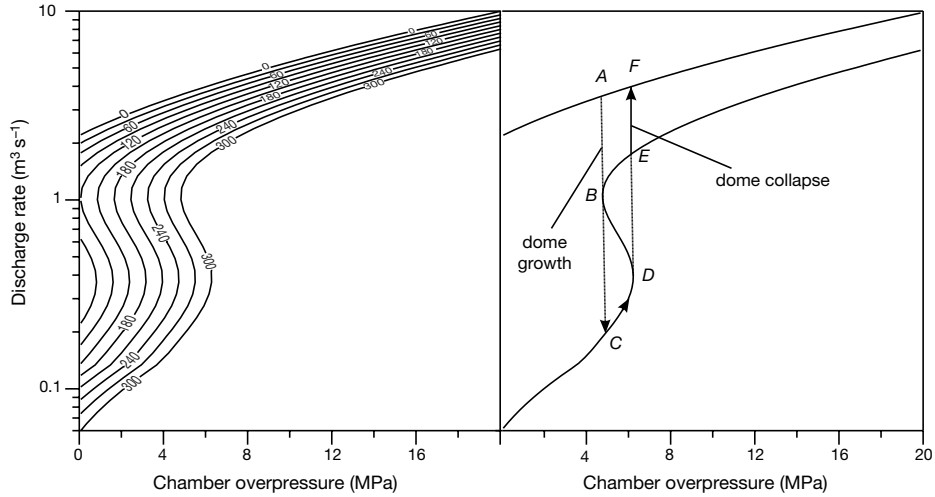

Figure 4 The relationship between extrusion rate and magma chamber pressure (**a**) and possible paths of unsteady eruption (**b**). Contours in **a** are of dome height from 0 to 300 m. See text for details about points A–F.

Received 4 June; accepted 27 September 1999.

1. Eichelberger, J. C., Carrigan, C. R., Westrich, H. R. & Price, R. H. Non-explosive silicic volcanism. *Nature* **323,** 598–602 (1986).
2. Sparks, R. S. J. Causes and consequences of pressurisation in lava dome eruptions. *Earth Planet. Sci. Lett.* **150,** 177–189 (1997).
3. Voight, B. *et al.* Magma flow instability and cyclic activity at Soufriere Hills Volcano, Montserrat, B.W.I. *Science* **283,** 1138–1142 (1999).
4. Hess, K. U. & Dingwell, D. B. Viscosities of hydrous leucogranite melts: a non-Arrhenian model. *Am. Mineral.* **81,** 1297–1300 (1996).
5. Lejeune, A. M. & Richet, P. Rheology of crystal-bearing melts: an experimental study at high viscosities. *J. Geophys. Res.* **100,** 4215–4229 (1995).
6. Stasiuk, M. V., Jaupart, C. & Sparks, R. S. J. Variations of flow rate and volume during eruption of lava. *Earth Planet. Sci. Lett.* **114,** 505–516 (1993).
7. Jaupart, C. & Allegre, C. J. Gas content, eruption rate and instabilities of eruption regime in silicic volcanoes. *Earth Planet. Sci. Lett.* **102,** 413–429 (1991).
8. Woods, A. W. & Koyaguchi, T. Transitions between explosive and effusive eruption of silicic magmas. *Nature* **370,** 641–645 (1994).
9. Stix, J. *et al.* A model for vulcanian eruptions at Galeras volcano, Colombia. *J. Volcanol. Geotherm. Res.* **77,** 285–304 (1997).
10. Young, S. R. *et al.* Overview of the Soufriere Hills Volcano and the eruption. *Geophys. Res. Lett.* **25,** 3389 (1998).
11. Young, S. R. *et al.* Monitoring SO_2 emission at the Soufriere Hills volcano: implications for changes in eruptive conditions. *Geophys. Res. Lett.* **25,** 3681–3684 (1998).
12. Boudon, G., Villemant, B., Komorowski, J. C., Idefonse, P. & Semet, M. P. The hydrothermal system at the Soufriere Hills Volcano, Montserrat (West Indies): Characterisation and role in the ongoing eruption. *Geophys. Res. Lett.* **25,** 3693–3696 (1998).
13. Fink, J. H., Anderson, S. W. & Manley, C. R. Textural constraints on effusive silicic volcanism. *J. Geophys. Res.* **97,** 9073–9083 (1992).
14. Klug, C. & Cashman, K. V. Permeability development in vesiculating magmas: implications for fragmentation. *Bull. Volcanol.* **58,** 87–100 (1996).
15. Dowty, E. in *Physics of Magmatic Processes* (ed. Hargreaves, R. B.) 419–485 (Princeton Univ. Press, 1980).
16. Lofgren, G. in *Physics of Magmatic Processes* (ed. Hargreaves, R. B.) 485–551 (Princeton Univ. Press, 1980).
17. Sohn, H. Y. & Moreland, C. The effect of particle size distribution on packing density. *Can. J. Chem. Eng.* **46,** 162–167 (1968).
18. Shepherd, J., Herd, R. A., Jackson, P. & Watts, R. Ground deformation measurements at the Soufriere Hills Volcano, Montserrat, 2, Rapid static GPS measurements. June 1996–June 1997. *Geophys. Res. Lett.* **25,** 3413–3416 (1998).
19. Miller, A. D. *et al.* Seismicity associated with dome growth and collapse of the Soufriere Hills Volcano, Montserrat. *Geophys. Res. Lett.* **25,** 3401–3405 (1998).
20. Nakada, S., Shimizu, H. & Ohta, K. Overview of the 1990–1995 eruption at Unzen Volcano. *J. Volcanol. Geotherm. Res.* **89,** 1–22 (1999).
21. Matthews, S. J., Gardeweg, M. C. & Sparks, R. S. J. The 1984–1996 cyclic activity of Lascar volcano, Northern Chile: cycles of dome growth, dome subsidence, degassing and explosive eruptions. *Bull. Volcanol.* **59,** 72–82 (1997).
22. Adilbirov, M. & Dingwell, D. B. High temperature fragmentation of magma by rapid decompression. *Nature* **380,** 146–149 (1996).
23. Young, S. R. *et al. Dome Collapse and Vulcanian Explosive Activity, September to October 1997* 1–23 (Special Rep. No. 5, Montserrat Observatory, Mongo Hill, Montserrat, 1999).
24. Sparks, R. S. J. *et al.* Magma production and growth of the lava dome of the Soufriere Hills volcano, Montserrat: November 1995 to December 1997. *Geophys. Res. Lett.* **25,** 3421–3424 (1998).
25. Murphy, M. D., Sparks, R. S. J., Barclay, J., Carroll, M. R. & Brewer, T. S. Remobilisation origin for andesite magma by intrusion of mafic magma at the Soufriere Hills Volcano, Montserrat, W.I., a trigger for renewed eruption. *J. Petrol.* (in the press).
26. Cashman, K. V. Groundmass crystallization of Mount St Helens dacite, 1980–1986: a tool for interpreting shallow magmatic processes. *Contrib. Mineral. Petrol.* **109,** 431–449 (1992).
27. Nakada, S. & Motomura, Y. Petrology of the 1991–1995 eruption at Unzen: effusion pulsation and groundmass crystallization. *J. Volcanol. Geotherm. Res.* **89,** 173–196 (1999).
28. Hammer, J. E., Cashman, K. V., Hoblitt, R. P. & Newman, S. Degassing and microlite crystallization during pre-climatic events of the 1991 eruption of Mt. Pinatubo, Philippines. *Bull. Volcanol.* **60,** 355–380 (1999).
29. Rose, W. I. Pattern and mechanism of volcanic activity at Santiaguito volcanic dome, Guatemala. *Bull. Volcanol.* **37,** 73–94 (1973).
30. Swanson, D. A. & Holcomb, R. T. *Lava Flows and Domes: Emplacement Mechanisms and Hazards Implications* (ed. Fink, J. H.) 3–24 (Springer, Berline, 1990).
31. Denlinger, R. & Hoblitt, R. P. Cyclic eruptive behaviour of silicic volcanoes. *Geology* **27,** 459–462 (1999).
32. Aspinall, W. P. *et al.* Soufriere Hills eruption, Montserrat: 1995–1997: volcanic earthquake locations and fault plane solutions. *Geophys. Res. Lett.* **25,** 3397–3400 (1998).
33. Barclay, J. *et al.* Experimental phase equilibria: constraints on pre-eruptive storage conditions of the Soufriere Hills magma. *Geophys. Res. Lett.* **25,** 3437–3440 (1998).
34. Devine, J. D., Rutherford, M. J. & Gardner, J. C. Petrologic determination of ascent rates for the 1995–1997 Soufriere Hills Volcano andesite magma. *Geophys. Res. Lett.* **25,** 3673–3676 (1998).

Acknowledgements

We thank H. Huppert, H. Mader and A. Woods for comments, and J. Fink and K. Cashman for criticisms and suggestions. This work was supported by the NERC, the Russian Foundation for Basic Research, and an NERC fellowship (R.S.J.S.).

Correspondence and requests for materials should be addressed to R.S.J.S. (e-mail: Steve.Sparks@bris.ac.uk).